TOXICOLOGICAL SCIENCES **115(1)**, 183–193 (2010)
doi:10.1093/toxsci/kfq032
Advance Access publication February 8, 2010

Mice Treated with Chlorpyrifos or Chlorpyrifos Oxon Have Organophosphorylated Tubulin in the Brain and Disrupted Microtubule Structures, Suggesting a Role for Tubulin in Neurotoxicity Associated with Exposure to Organophosphorus Agents

Wei Jiang,* Ellen G. Duysen,* Heidi Hansen,* Luda Shlyakhtenko,† Lawrence M. Schopfer,* and Oksana Lockridge*,[1]

*Eppley Institute, University of Nebraska Medical Center, Omaha, Nebraska 68198-5950; and †Department of Pharmaceutical Sciences, University of Nebraska Medical Center, Omaha, Nebraska 68198-6025

[1] To whom correspondence should be addressed. Fax: (402) 559-4651. E-mail: olockrid@unmc.edu.

Received November 30, 2009; accepted January 22, 2010

Exposure to organophosphorus (OP) agents can lead to learning and memory deficits. Disruption of axonal transport has been proposed as a possible explanation. Microtubules are an essential component of axonal transport. *In vitro* studies have demonstrated that OP agents react with tubulin and disrupt the structure of microtubules. Our goal was to determine whether *in vivo* exposure affects microtubule structure. One group of mice was treated daily for 14 days with a dose of chlorpyrifos that did not significantly inhibit acetylcholinesterase. Beta-tubulin from the brains of these mice was diethoxyphosphorylated on tyrosine 281 in peptide GSQQY$_{281}$RALTVPELTQQMFDSK. A second group of mice was treated with a single sublethal dose of chlorpyrifos oxon (CPO). Microtubules and cosedimenting proteins from the brains of these mice were visualized by atomic force microscopy nanoimaging and by Coomassie blue staining of polyacrylamide gel electrophoresis bands. Proteins in gel slices were identified by mass spectrometry. Nanoimaging showed that microtubules from control mice were decorated with many proteins, whereas microtubules from CPO-treated mice had fewer associated proteins, a result confirmed by mass spectrometry of proteins extracted from gel slices. The dimensions of microtubules from CPO-treated mice (height 8.7 ± 3.1 nm and width 36.5 ± 15.5 nm) were about 60% of those from control mice (height 13.6 ± 3.6 nm and width 64.8 ± 15.9 nm). A third group of mice was treated with six sublethal doses of CPO over 50.15 h. Mass spectrometry identified diethoxyphosphorylated serine 338 in peptide NS$_{338}$NFVEWIPNNVK of beta-tubulin. In conclusion, microtubules from mice exposed to chlorpyrifos or to CPO have covalently modified amino acids and abnormal structure, suggesting disruption of microtubule function. Covalent binding of CPO to tubulin and to tubulin-associated proteins is a potential mechanism of neurotoxicity.

Key Words: **chlorpyrifos; tubulin; mass spectrometry; nanoimaging; neurotoxicity.**

Organophosphorus (OP) agents are used as pesticides, in jet engine oil as a flame retardant, as chemical warfare agents, and for treatment of Schistosomiasis. The acute toxicity that occurs with high doses of OP is due to inhibition of acetylcholinesterase (AChE). Some people who survive acute exposure describe neurological symptoms that last long after the acute symptoms have abated. The sarin attack in the Tokyo subway occurred in 1995, but 5 years later, some victims of this attack still suffered from blurred vision, easy fatigability, difficulty in concentration, and insomnia (Kawada *et al*., 2005; Yanagisawa *et al*., 2006). Magnetic resonance imaging revealed structural changes in the brains of exposed subjects (Yamasue *et al*., 2007). These long-lasting symptoms could be the consequence of seizure activity and anoxia initiated by acute inhibition of AChE (McDonough and Shih, 1997).

Low doses of OP that do not inhibit AChE have also been associated with neurological dysfunction, including clinically significant extrapyramidal symptoms, anxiety, depression (Salvi *et al*., 2003), memory loss, and learning disability (Srivastava *et al*., 2000). The mechanism of low-dose toxicity is not understood. One hypothesis to explain long-lasting neurotoxicity from low doses of OP involves OP modification of proteins in the axonal transport system (Gearhart *et al*., 2007; Gupta *et al*., 1997; Prendergast *et al*., 2007; Terry *et al*., 2007). The transport system moves organelles from the cell nucleus to the axon termini and back to the nucleus. Hundreds of proteins are present in the axoplasm of neurons (Rishal *et al*., 2010), suggesting the involvement of a great many proteins in this transport process.

Indirect evidence supports the hypothesis that organophosphorylation of key proteins in the axonal transport system disrupts the transport mechanism in neurons (Gearhart *et al*., 2007; Terry *et al*., 2007). Such a disruption could result in loss of synaptic contacts, slow dying back of axon structures, and finally in neuron cell death as has been described by Morfini *et al*. (2009) to explain neurodegenerative diseases, including Parkinson's, Alzheimer's disease, and amyotrophic lateral sclerosis.

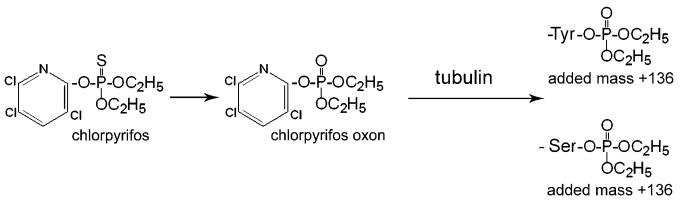

FIG. 1. Chlorpyrifos is bioactivated to CPO by cytochrome P450. Results presented below show that the oxon reacts with tubulin by donating its diethoxyphosphate group to tyrosine 281 and to serine 338 of beta-tubulin in mouse brain. Each diethoxyphosphate group adds a mass of 136 amu to tubulin. The 3,5,6-trichloro-2-(*O*)-pyridine group is released from CPO and excreted.

Rats treated chronically with low doses of chlorpyrifos have decreased rates of axonal transport measured in sciatic nerves *ex vivo*, implicating OP modification of tubulin, kinesin, and microtubule-associated proteins in this dysfunction (Gearhart *et al*., 2007; Terry *et al*., 2007). The present report focuses on tubulin in brain because *in vitro* experiments have shown that OP modification of tubulin disrupts polymerization of tubulin into microtubules (Grigoryan and Lockridge, 2009; Prendergast *et al*., 2007). Disruption of tubulin polymerization has been shown to result in neuron dysfunction, cellular apoptosis, and tissue damage (Conde and Caceres, 2009; Tierno *et al*., 2009).

Mass spectrometry analysis of a variety of proteins treated with OP *in vitro* identified covalent binding of OP to tyrosine and lysine residues (Grigoryan *et al*., 2008, 2009a,b,c). The results suggest that almost any protein can be modified by OP. Previously, OP adducts were thought to form only with the active site serine of enzymes in the serine hydrolase superfamily. *In vivo* studies have identified OP-tyrosine adducts in the blood of guinea pigs treated with nerve agents and have shown that the adducts are detectable 24 days after exposure at a time when OP-serine adducts of butyrylcholinesterase (BChE) are no longer detectable (Read *et al*., 2010).

In the present report, we treated mice with the pesticide chlorpyrifos as well as with its active metabolite, chlorpyrifos oxon (CPO). The pesticide chlorpyrifos is relatively harmless to man and rodents because it is rapidly detoxified and excreted. However, a portion of the chlorpyrifos is bioactivated through oxidative desulfuration catalyzed by cytochrome P450 enzymes to form CPO, the toxic agent that inhibits AChE (Sams *et al*., 2004; Tang *et al*., 2001) (see Fig. 1).

Our goal was to identify alterations in microtubule structure following *in vivo* treatment of mice with chronic low doses of chlorpyrifos and with sublethal doses of CPO. This is the first report to identify structural deficits in microtubules of animals treated *in vivo* with OP and furthermore to provide mass spectrometry evidence for OP labeling of tubulin in mice treated *in vivo* with chlorpyrifos or CPO.

MATERIALS AND METHODS

Materials. Chlorpyrifos and CPO (PS-674 and MET-674B; ChemService Inc., West Chester, PA) were stored at −80°C. Guanosine 5′-triphosphate (GTP) sodium salt hydrate (G8877) ≥ 95% HPLC pure powder and 1,4-piperazinediethanesulfonic acid (PIPES, P6757) > 99% pure powder were from Sigma (St Louis, MO). Sequencing grade–modified trypsin (V5113) was from Promega (Madison, WI). Alpha-cyano-4-hydroxycinnamic acid was from Applied Biosystems (MDS Sciex; Foster City, CA). All other chemicals were of analytical grade.

Animal. All animal work was conducted in accordance with the Guide for the Care and Use of Laboratory Animals as adopted by the National Institutes of Health. Formal approval to conduct the experiments was obtained from the Institutional Animal Care and Use Committee of the University of Nebraska Medical Center. Adult wild-type mice of strain 129Sv were used in all trials. Mice were bred at the University of Nebraska Medical Center.

Adult female mice treated for 14 days with a low dose of chlorpyrifos ($n = 4$) (85.6 ± 11.2 days of age) weighed an average of 19.8 ± 3.2 g, while female control mice ($n = 4$) (90.1 ± 5.8 days of age) weighed an average of 18.2 ± 1.4 g. Adult male mice treated with a single sublethal dose of CPO ($n = 3$) (72 days of age) weighed an average of 24.6 ± 1.4 g, and control male mice ($n = 3$) (72 days of age) weighed an average of 23.8 ± 1.9 g. Two female mice were treated with six sublethal doses of CPO over a period of 50.15 h (127 days of age, 23.0 g), and two control female mice (127 days of age, 22.6 g) were treated at the same time points with an equivalent volume of ethanol.

Chronic low-dose treatment of mice (n = 4) with chlorpyrifos. Female mice ($n = 4$) were injected sc with 3 mg/kg chlorpyrifos dissolved in 3% dimethyl sulfoxide/97% corn oil. Each mouse was treated for 14 consecutive days between 10 and 11 A.M. Surface body temperature, body weight, and observations were made every 5 min through 15 min and at 30-min postdosing. The axial body temperature was measured with a digital thermometer, Thermalert model TH-5, and a surface Microprobe MT-D, Type T thermocouple (Physitemp Instruments Inc., Clifton, NJ). Blood was collected (50 µl) via the saphenous vein prior to dosing each day. On day 15, 24 h after the final dose, the mice were decapitated, plasma was collected, and the brains placed on ice. Brains were weighed and processed according to the tubulin purification protocol. The tubulin was examined for OP modifications.

Single-dose treatment of mice (n = 3) with chlorpyrifos. In three separate experiments, a mouse was injected ip with CPO dissolved in ethanol at a dose of 3.0 mg/kg delivered in 50 µl. A control mouse was injected with ethanol only. Animals were observed for signs of toxicity following injection. About 30-min postinjection, the mice were euthanized and perfused with 50 ml of 0.1M PBS to remove blood from tissues. Tubulin from the brains of these animals was purified and used for nanoimaging and SDS gel electrophoresis. Proteins in the SDS bands were analyzed mass spectrally.

Treatment of mice (n = 2) with six doses of CPO. To derive samples for mass spectral analysis of CPO-labeled tubulin, mice ($n = 2$) were injected ip with CPO dissolved in ethanol at a dose of 2.5 mg/kg delivered in 50 µl. Control mice ($n = 2$) were injected with ethanol only. Each mouse received six injections at 0, 1, 22, 48, 50, and 50.15 h. Animals were observed for signs of toxicity after each injection. Mice were euthanized 5 min after the last dose by inhalation of carbon dioxide and then perfused via intracardial injection with 50 ml 0.1M PBS solution to remove blood from the tissues. Tubulin from the brains of these animals was examined for OP modifications.

Enzyme activity assays. AChE and BChE activities in mouse plasma and brain were measured with 1mM acetylthiocholine and 1mM butyrylthiocholine, respectively, as described (Peeples *et al*., 2005). Carboxylesterase activity in mouse plasma was assayed with 2.5mM *p*-nitrophenyl acetate after incubating 3 µl plasma for 5 min in 0.1M potassium phosphate (pH 7.0) containing 12.5mM EDTA, to inhibit paraoxonase, and 0.01mM eserine, to inhibit AChE and BChE. The reaction was started by adding 0.05 ml of 0.1M *p*-nitrophenyl acetate dissolved in methanol. The total reaction volume was 2.0 ml, and the temperature was 25°C. Absorbance increase at 400 nm was measured on a Gilford spectrophotometer and recorded on a computer interfaced to MacLab/200 (AD Instruments, Sydney, Australia). Activity in micromoles per minute was calculated from the extinction coefficient for *p*-nitrophenol of $9000 M^{-1} cm^{-1}$.

Tubulin purification and polymerization. Tubulin from mouse brains was purified by two cycles of polymerization using the protocol of Shelanski *et al.* (1973). Brains from mice were collected and placed on ice. The brains were homogenized in four volumes of ice-cold PM buffer (80mM PIPES, 2mM magnesium chloride, and 0.5mM ethylene glycol tetraacetic acid (EGTA), pH 7.0) and centrifuged at 17,000 × g for 60 min at 4°C. The pellet was discarded, and the clear supernatant was transferred to a clean ultracentrifuge tube. The supernatant, in which no microtubules were present, was mixed with an equal volume of 8M glycerol containing 1.0mM GTP. The samples were incubated for 2 h at 37°C to assemble the microtubules. The solution was centrifuged for 60 min at 100,000 × g at 29°C to pellet the microtubules and remove the polymerization inducers glycerol and GTP. The pellet was suspended in 500 µl PM buffer, depolymerized on ice for 30 min, and centrifuged for 1 h at 4°C to remove particulates. Tubulin in the supernatant was mixed with an equal volume of 8M glycerol containing 1.0mM GTP and incubated for 45 min at 37°C to assemble the microtubules for a second time. The sample was centrifuged for 60 min at 29°C to pellet the microtubules. The pellet was resuspended in 1 ml of PM buffer and maintained at room temperature to preserve the microtubules. The protein concentration of the final microtubule pellet ranged from 3 to 7 µg/µl (depending on the preparation) as measured by absorbance at 280 nm using the NanoDrop spectrophotometer ND-1000 (NanoDrop Technologies Inc.; Thermo Scientific, Waltham, MA). Absorbance at 280 nm was compared to protein concentration estimated from the Pierce bicinchoninic acid protein assay. Both methods gave similar results. Bovine albumin was used as the standard for both assays.

Atomic force microscopy of microtubules. Atomic force microscopy nanoimages were acquired in the Nanoimaging Core Facility at the University of Nebraska Medical Center, codirected by L.S. A portion of the microtubule pellet, prepared by two cycles of assembly, was fixed immediately by addition of glutaraldehyde to 0.25%. The fixed microtubules were stored at 4°C for 12 h before an aliquot was diluted 10-fold with double-distilled water to a protein concentration of 0.5 µg/µl. Ten microliters of the suspension was drawn from the bottom of the tube and placed in the center of a mica chip that had been treated with 1-(3-aminopropyl) silatrane. The detailed procedure for mica surface modification is given in Shlyakhtenko *et al.* (2003) and Lyubchenko and Shlyakhtenko (2009). The silatrane modification allows the sample to be deposited in a wide range of ionic strengths and pH. After 2-min incubation in a humid chamber, the samples were rinsed with deionized water and dried with argon gas flow. Images were acquired using an MFP-3DAtomic Force Microscope (Asylum Research, Santa Barbara, CA) operated in tapping mode. Pictures were taken from 15 different 5 × 5 µm areas on average. Image processing and measurement of microtubule height and width were performed using Femtoscan software (Advanced Technology Center, Moscow, Russia).

Off-line HPLC purification of peptides for determination of labeled proteins by mass spectrometry. A portion of the microtubule pellet was denatured in 8M urea, reduced with 10mM dithiothreitol, and carbamidomethylated with 50mM iodoacetamide. The sample was diluted to 2M urea and then digested with trypsin at a ratio of 50:1 (wt/wt) at 37°C for 16 h. The salt concentration was reduced by dilution rather than by dialysis because dialysis resulted in loss of up to 95% of the tubulin protein due to sticking to the dialysis membrane. Peptides were desalted and separated by reverse phase HPLC on a 100 × 4.60 mm Phenomenex C18 column eluted with a gradient from 0 to 60% (vol/vol) acetonitrile versus 0.1% (vol/vol) trifluoroacetic acid at a flow rate of 1 ml/min for 60 min on a Waters 625 LC system. Fractions of 1 ml were collected, dried by vacuum centrifugation, and redissolved in 50 µl of 5% acetonitrile and 0.1% formic acid. Fractions that eluted between 5 and 40 min were analyzed by liquid chromatography-tandem mass spectrometry (LC-MSMS) electrospray ionization. The CPO-labeled peptide in Figure 4 was in fraction 38, and the CPO-labeled peptide in Figure 7 was in fraction 30. Details on the method for searching mass spectrometry data to identify labeled peptides are in the "Materials and Methods" section entitled Q-Trap 4000 and LTQ-Orbitrap mass spectrometry. In brief, the mass spectrometry data were compared to the National Center for Biotechnology Information (NCBI) nonredundant database using Mascot software. Diethoxyphosphate was used as a variable modification for Ser, Thr, Tyr, and Lys. Each identified peptide was manually examined to verify that the tandem mass spectral fragmentation (MSMS) spectrum supported the Mascot assignment.

Polyacrylamide gel electrophoresis of proteins in the microtubule pellet, followed by in-gel digestion. Two gradient polyacrylamide gels (4–30%) were cast in a Hoefer gel apparatus to make 15 × 11–cm gels, 0.75-mm thick, with a single well that spanned the entire gel. Microtubule pellets from control and CPO-treated mouse brains in 400 µl PM buffer were denatured by addition of 80 µl of 6 × SDS gel loading buffer containing 0.2M Tris/Cl (pH 6.8), 10% SDS, 30% glycerol, 0.6M dithiothreitol, and 0.012% bromophenol blue. The samples were boiled for 3 min, and each was loaded onto a gel. About 2 mg of protein were loaded onto each gel. Electrophoresis was for 3000 V/h at 4°C. Gels were stained with Coomassie blue. Protein bands from the upper 75% of each gel were cut into slices. Gel slices were destained, dried, treated with trypsin, and the peptides extracted as previously described (Peeples *et al.*, 2005). The dry samples were dissolved in 80 µl of 5% acetonitrile and 0.1% formic acid and placed in autosampler vials for analysis in the Q-Trap 4000 (MDS Sciex; Applied Biosystems) and the LTQ-Orbitrap (Thermo Scientific) mass spectrometers.

Q-Trap 4000 and LTQ-Orbitrap mass spectrometry. Peptides purified by off-line HPLC or extracted from gel slices were analyzed by LC-MSMS in the Q-Trap 4000 linear ion trap mass spectrometer using a nanospray source with a continuous flow head, at a flow rate of 0.3 µl/min (Li *et al.*, 2009). The four most intense peptides in each cycle of analysis were fragmented by collision-induced dissociation using pure nitrogen at 40 µ Torr and a collision energy of 20–50 V. Collision voltage was determined by the Analyst software based on the size and charge state of the peptide. The data were searched against the NCBI nonredundant database using Mascot v 1.9 (Matrix Science Ltd, London, UK) for tryptic peptides with an added mass of 136 Da from CPO (Perkins *et al.*, 1999). The CPO added mass was put into the UNIMOD public database of protein modifications (http://www.unimod.org) for use with Mascot. Mascot search parameters included peptides with one missed tryptic cleavage, carbamidomethylated cysteine as a fixed modification; diethoxyphosphorylated serine, threonine, tyrosine, and lysine; and oxidized methionine as variable modifications, a peptide mass tolerance of 1.2 Da and a fragment mass tolerance of 0.6 Da. The MSMS fragmentation spectra of peptides identified by Mascot were manually confirmed with the aid of the MS-Product algorithm from Protein Prospector (v 5.3.2 from the University of California Mass Spectrometry Facility). Peptides extracted from gel slices were also analyzed in the LTQ-Orbitrap mass spectrometer as described (Wiederin *et al.*, 2009).

Statistical analysis of microtubule nanoimaging parameters. A two-independent sample *t*-test was performed to determine the statistical significance of differences in the dimensions of the microtubules between the treated and control groups. The data were normally distributed. SPSS software 16.0 (Microsoft Corp., Redmond, WA) was used for statistical analysis.

RESULTS

Mice Treated Chronically with Low Doses of Chlorpyrifos

Nontoxic dose of chlorpyrifos. Mice injected daily for 14 consecutive days with a nontoxic dose of chlorpyrifos (not the oxon), 3 mg/kg sc, showed no signs of toxicity with the exception of hunched posture, which persisted for less than 15 min after treatment. Their body temperature and body weight remained normal (see Fig. 2).

Plasma AChE activity dropped from 0.3 to 0.2 U/ml after the first two doses of chlorpyrifos but rebounded to 0.45 U/ml after 9–14 days of treatment (see Fig. 3A). In contrast, plasma BChE

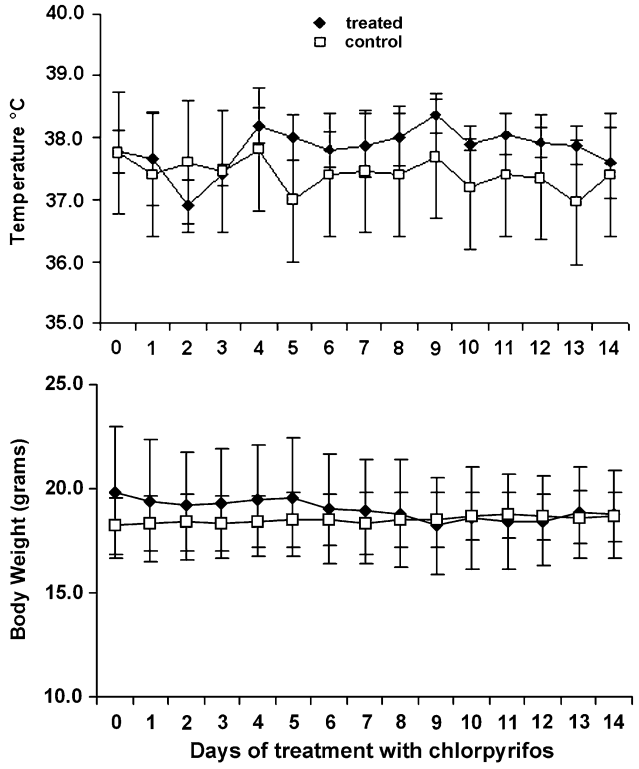

FIG. 2. Surface body temperature and body weight of mice treated daily for 14 days sc with 3 mg/kg chlorpyrifos (not the oxon). Values for control mice ($n = 4$) treated with vehicle were indistinguishable from values for treated mice ($n = 4$). Day 0 values are the temperature and body weight before treatment. Errors bars are SD.

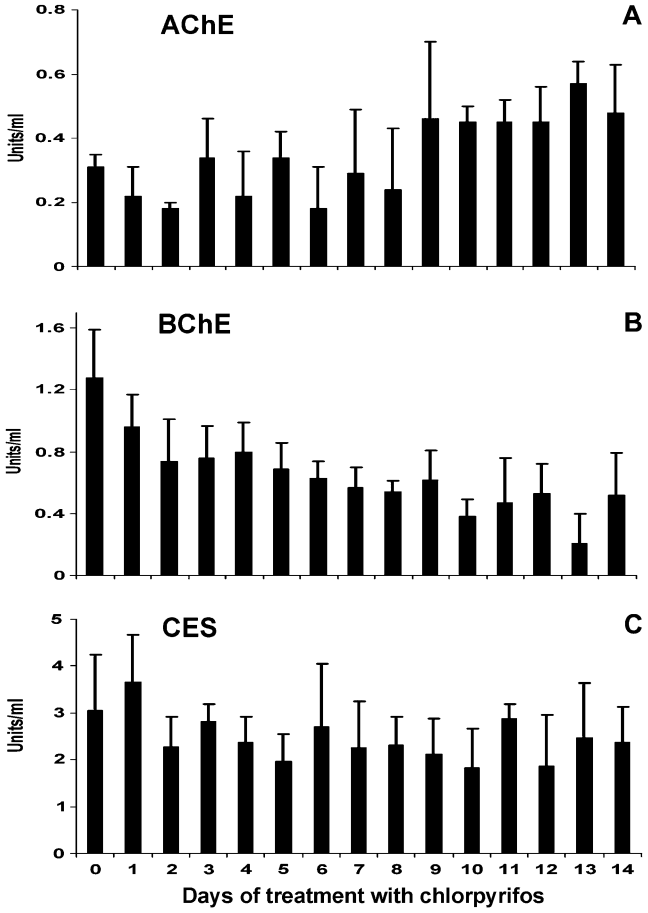

FIG. 3. Plasma esterase activity in mice ($n = 4$) treated daily for 14 days with chlorpyrifos, 3 mg/kg sc. (A) Plasma AChE activity. (B) Plasma BChE activity. (C) Plasma carboxylesterase (CES) activity. Day 0 values are the activities before treatment was begun. Units of activity are micromoles substrate hydrolyzed per minute per microliter plasma. Error bars are SD for four mice.

activity steadily declined following each injection of chlorpyrifos (Fig. 3B). This result is consistent with the greater sensitivity of BChE to inhibition by CPO compared to that of AChE (Amitai *et al*., 1998). Plasma carboxylesterase activity was unaffected (Fig. 3C). Since inhibition of BChE has no health consequences and since AChE activity was not inhibited by the 14th day of treatment, it is concluded that the dosing regimen was nontoxic.

Mass spectrometry identifies CPO-modified tubulin. Tubulin purified from the brains of mice treated with a daily low dose of chlorpyrifos was digested with trypsin and analyzed by LC-MSMS. The mass spectrometry data were searched for diethoxyphosphorylated peptides with an added mass of 136 amu on tyrosine, serine, threonine, or lysine. One modified peptide was found. Figure 4 shows the MSMS spectrum for peptide $GSQQY_{281}RALTVPELTQQMFDSK$ from mouse beta-tubulin, covalently modified on tyrosine 281 by diethoxyphosphate. The triply charged parent ion has a mass-to-charge ratio of 854.8, which is consistent with the peptide sequence plus 136 amu from the diethoxyphosphate. The y5 to y11 ions and the internal fragments support the sequence. Internal fragments are at 157.0 (AL minus 28), 268.1 (ALT minus water), 286.2 (LTV minus 28), 367.1 (ALTV minus water), 423.0 (PELT minus water), 569.2 (PELTQ), 653.2 (LTVPEL), 697.2 (PELTQQ), 737.2 (QQMFDS), and 920.3 amu (YRALTVP diethoxyphosphorylated on Y).

Support for modification of tyrosine comes from the internal fragment at 920.3 amu, which corresponds to the sequence Y*RALTVP where Y has an added mass of 136 amu. The threonine in peptide YRALTVP can be ruled out as the site of diethoxyphosphorylation because internal fragments that include this threonine (ALT minus water, LTV minus 28, ALTV minus water, and LTVPEL) do not have an added mass of 136 amu. The second threonine in peptide $GSQQY_{281}RALTV$-PELTQQMFDSK can be ruled out because internal fragments that include this threonine (PELT minus water, PELTQ, and PELTQQ) do not have an added mass of 136 amu. The serine near the C-terminus can be ruled out based on the mass of the internal fragment QQMFDS. The serine near the N-terminal can be ruled out based on the mass of the doubly charged b4 ion. Precedent for the reactivity of this tyrosine in tubulin

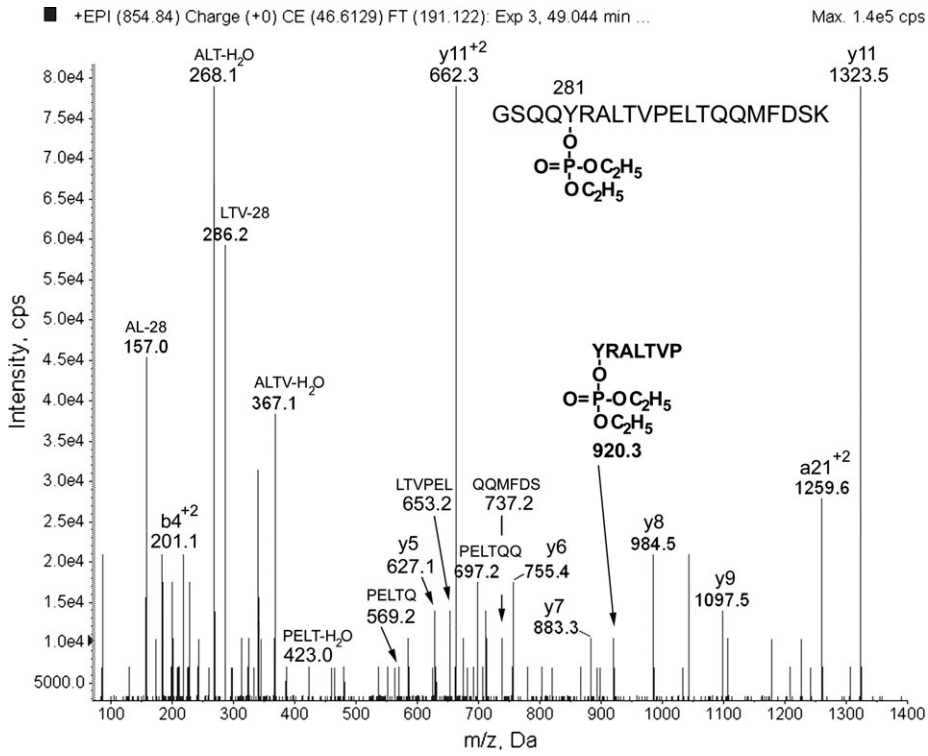

FIG. 4. Mouse beta-tubulin from brain, covalently modified after *in vivo* treatment with 14 daily low doses of chlorpyrifos that did not significantly inhibit AChE activity. The triply charged parent ion has a mass-to-charge ratio (*m*/*z*) of 854.8. The masses of the y ions and the internal cleavage ions are consistent with the sequence GSQQY_{281}RALTVPELTQQMFDSK (accession number gi 21746161) where the diethoxyphosphorylated residue is tyrosine 281. The presence of the internal cleavage ion at 920.3 amu is direct evidence that the modification is on tyrosine.

comes from *in vitro* experiments where the homologous tyrosine in bovine beta-tubulin, GSQQY_{281}R, was covalently labeled by CPO (Grigoryan *et al*., 2009c).

Mice Treated with a Single Dose of CPO

Signs of toxicity. Mice treated ip with one dose of 3.0 mg/kg CPO and euthanized 30-min postdosing had toxic signs, including decreased body temperature (average reduction 2.1°C ± 0.5), reduced activity, piloerection, and hunched posture. BChE and AChE activities in the plasma were inhibited 70 and 62%, respectively. Tubulin from the brains of these mice was purified and polymerized to microtubules. The proteins in an aliquot of these microtubules were separated by SDS gel electrophoreses and identified by mass spectrometry. Another aliquot of the microtubule preparation was used for nanoimaging.

CPO-treated mice have decreased levels of proteins that cosediment with microtubules. Figure 5 shows the SDS gels stained with Coomassie blue from which gel slices were analyzed by mass spectrometry. The banding pattern and staining intensities are similar for the control and treated samples. The original goal of this experiment was to identify proteins modified by CPO. In anticipation that several proteins would be modified by CPO, gel slices from the upper 75% of the gels were prepared for mass spectrometry. The criterion for a positive result was finding the labeled peptide and finding an MSMS spectrum that supported the presence of diethoxyphosphate in the peptide. Labeled peptides are extremely difficult to find. The LC-MSMS analysis identified the proteins in the gel slices but did not identify any labeled peptides. However, the mass spectrometry analysis showed the surprising result that the set of proteins was not identical in the two gels. The microtubules from the CPO-treated mice were missing the six proteins listed at the bottom of Table 1. The missing proteins were well represented in the control microtubule sample but were undetectable in microtubules prepared from CPO-treated mice.

The Coomassie-stained bands in the gels in Figure 5 appeared identical, yet mass spectrometry analysis of the proteins in the gels revealed missing proteins in the microtubules from the CPO-treated mouse. This result can be explained by the fact that any gel slice contains multiple proteins. Coomassie blue staining reports the aggregate composition of the band, favoring the most abundant proteins, but mass spectrometry identifies the individual proteins in a gel band.

The mass spectrometry results in Table 1 are supported by the atomic force microscopy nanoimages in Figure 6. Microtubules prepared from control mouse brain in Figure 6A are

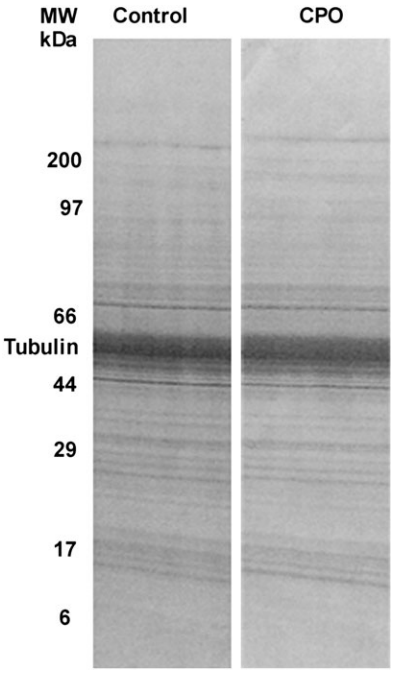

FIG. 5. Coomassie blue–stained SDS gels. Tubulin isolated from the brains of control and CPO-treated mice was polymerized to microtubules. The microtubule preparations were denatured and loaded on the gels. Each 15-cm wide gel was loaded with 2 mg of protein. A representative 1.5-cm portion of each gel is shown. The upper 75% of each gel was sliced horizontally. Proteins were extracted from the gel slices, digested with trypsin, and analyzed by mass spectrometry.

decorated with many proteins. In contrast, microtubules prepared from the CPO-treated mouse brain in Figure 6B have few attached proteins.

The microtubules from CPO-treated animals (in Fig. 6B) appeared to be thinner than those from untreated animals (in Fig. 6A). The difference was quantified by measuring the width and height of 100 microtubules at three to four positions along each tubule for a total of 700 measurements. Figure 6C shows that the average width was 64.8 ± 15.9 nm for the control and 36.5 ± 15.5 nm for the CPO-treated microtubules. The average height was 13.6 ± 3.6 nm for the control and 8.7 ± 3.1 nm for the CPO-treated microtubules.

The atomic force microscopy nanoimaging and the mass spectrometry experiments to identify proteins that cosediment with microtubules were conducted by two researchers, each finding similar results. It is unlikely that the missing proteins were removed during purification as both control and CPO-treated samples were handled identically, and the tubulin was not exposed during the purification process to the high-salt conditions, which remove microtubule-associated proteins (Friden and Wallin, 1991).

TABLE 1
Proteins Identified in Control and CPO-Treated Mouse Brain Microtubules

Protein	Molecular weight (kDa)	Accession number	Control Mowse score	CPO Mowse score
Plectin 1 isoform 6	534	gi 41322931	78	110
Dynein, cytoplasmic, heavy chain 1	527	gi 148686723	1254	589
Titin	300	gi 123232572	112	68
Microtubule-associated protein 1A	300	gi 122065442	913	841
Microtubule-associated protein 1B	271	gi 6678946	1066	1573
Microtubule-associated protein 2	199	gi 126741	4982	4769
Microtubule-associated protein 4	121	gi 148677083	423	271
mKIAA0325 protein	230	gi 28972155	1424	790
Neurofilament protein	115	gi 200022	964	295
Mtap4 protein	114	gi 29747932	432	308
Stop protein	96	gi 2769587	324	383
Ulip2 protein	62	gi 1915913	362	148
Neurofilament L	61	gi 387492	504	499
Tubulin beta 3	50	gi 12963615	600	672
Tubulin beta 1	50	gi 124430500	89	160
Tubulin beta 5	50	gi 7106439	826	803
Tubulin beta 6	50	gi 27754056	686	467
Tubulin alpha isotype *m*-alpha 2	50	gi 202210	923	522
Tubulin alpha 1C	50	gi 6678469	920	672
Tubulin alpha 1B	50	gi 34740335	571	550
Tubulin alpha 1a	50	gi 6678465	909	403
Alpha-tubulin	50	gi 74182829	256	330
Tubulin alpha 8	50	gi 8394493	502	125
Microtubule-associated protein tau	76	gi 13432200	739	374
Beta-tubulin	42	gi 202229	412	440
Tubulin polymerization–promoting protein	24	gi 33469051	401	417
Cytoskeleton-associated protein 5	218	gi 123227410	915	0
Myosin Va	215	gi 148694358	2097	0
Heat-shock protein 84 kDa	84	gi 309317	123	0
Dynein, cytoplasmic, 1 light intermediate chain	57	gi 22122795	422	0
Alpha-internexin	56	gi 94730353	543	0
Microtubule-associated protein 2 isoform 1	53	gi 90186270	396	0

Note. Accession number is the identifying number in the NCBI nonredundant protein database. Mowse scores are assigned by Mascot software to indicate the probability that the assignment is correct. They are the sum of the scores for all of the peptides associated with a particular protein. A score of 69 or higher is considered to be a definitive assignment ($p < 0.05$).

Mice Treated with Six Sublethal Doses of CPO

Signs of toxicity. Mice treated ip with six doses of 2.5 mg/kg CPO showed no toxic signs after injections at 0, 1, 22, 48, and 50 h. Following the injection at 50.15 h, CPO-treated mice had hunched posture, piloerection, decreased activity, ataxic gait, decrease in body temperature (average reduction 4.2°C ± 1.8), and lacrimation. Mice were euthanized 5 min after the 50.15-h

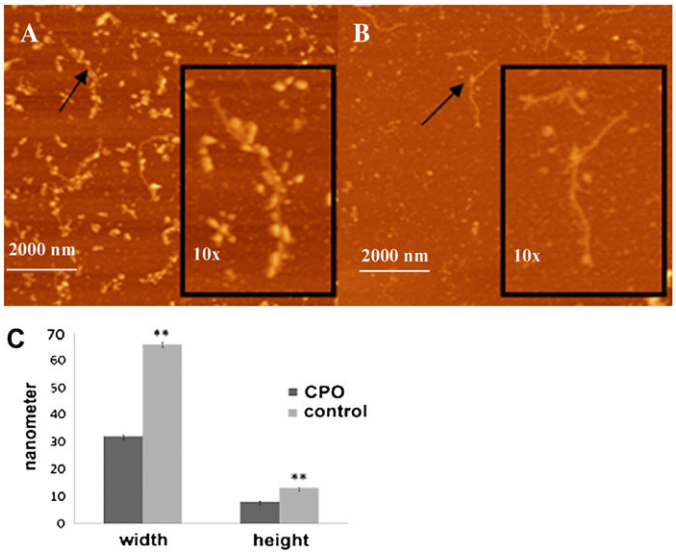

FIG. 6. Atomic force microscopy nanoimages of microtubules from purified mouse brain tubulin. (A) Microtubules from a control mouse. Microtubules are highly decorated with associated proteins. (B) Microtubules from a mouse treated ip with CPO (3 mg/kg). Microtubules show fewer associated proteins. Arrows indicate microtubules that are shown as magnified images in the box inserts. Mice were injected, and microtubules from both a control ($n = 3$) and a CPO ($n = 3$)-treated animal were prepared and imaged on three different occasions by two different investigators. All three trials gave similar results. (C) Width and height comparison for microtubules from CPO-treated and control groups. **Statistically significant difference ($p = 0.001$).

dosing. BChE and AChE plasma activities were completely inhibited 5 min after the 50.15-h injection. At this same time point, BChE and AChE activities in the brain were inhibited 50 and 46%, respectively. Brains from these mice were the source of the tubulin that yielded the CPO-labeled peptide in Figure 7.

Second tubulin peptide labeled by CPO Collision-induced fragmentation identified a second tubulin peptide covalently modified by CPO. The MSMS fragmentation spectrum in Figure 7 shows peptide NS_{338}NFVEWIPNNVK of beta-tubulin to be covalently modified on serine 338 by CPO. The masses of y and b ions exactly fit the indicated sequence. Internal fragments are at 430 (EWI), 538.3 (IPNNV), 584.3 (S_{338}NFV with diethoxyphosphate on S), and 740 amu (VEWIPN). Support for labeling on serine comes from the internal fragment at 584.3 amu, which corresponds to the sequence S_{338}NFV, where S has an added mass of 136 Da. In addition, the parent ion mass requires the presence of an extra 136 amu component, and there are no other nucleophilic residues in this peptide that could reasonably support reaction with CPO.

DISCUSSION

Tubulin Peptides Labeled by CPO in Living Mice

Living mice treated with a nontoxic dose of chlorypyrifos or a sublethal dose of CPO have CPO-labeled tubulin in their brains. The identification of two diethoxyphosphorylated tubulin residues (tyrosine 281 and serine 338) is direct evidence that CPO covalently reacts with tubulin in mouse brain.

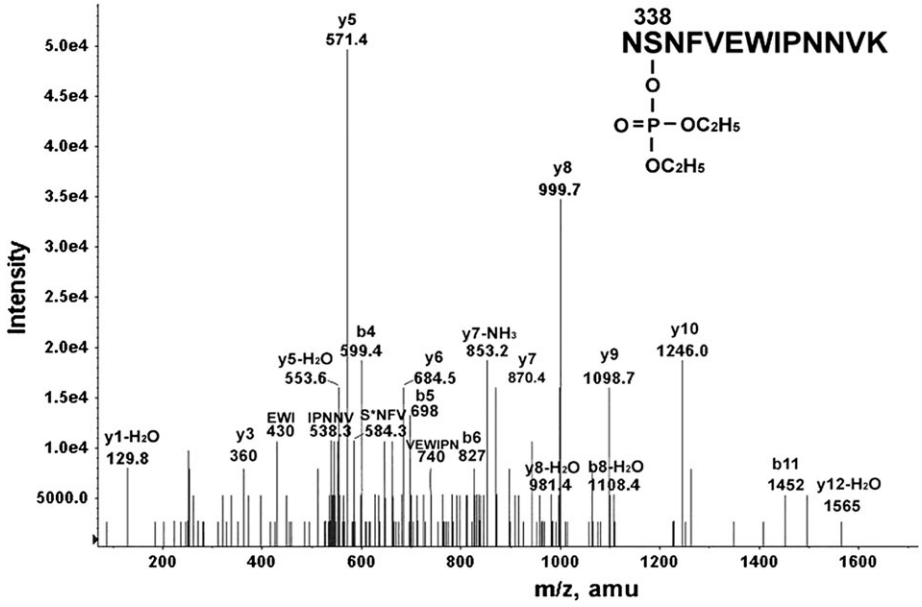

FIG. 7. MSMS fragmentation spectrum of the NS_{338}NFVEWIPNNVK peptide labeled by CPO on serine 338 of mouse beta-tubulin (accession number gi 91855). The doubly charged parent ion has a mass-to-charge ratio (m/z) of 849.0. The spectrum was acquired in the Q-Trap 4000 mass spectrometer. Mice had been treated with sublethal doses of CPO six times over a period of 50.15 h.

TABLE 2
CPO-Labeled Beta-Tubulin Peptides

Species	Sequence	Accession number	Labeled amino acid	Reference
Mus musculus	GSQQY$_{281}$RALTVPELTQQMFDSK	gi 21746161	Tyr 281	Present work
Bovine	GSQQY$_{281}$RALTVPELTQQMFDAK	gi 75773583	Tyr 281	Grigoryan *et al*. (2009c)
Homo sapiens	GSQQY$_{281}$RALTVPELTQQMFDSK	gi 4507729	Unknown	
Mus musculus	NS$_{338}$NFVEWIPNNVK	gi 91855	Ser 338	Present work
Bovine	NSSY$_{340}$FVEWIPNNVK	gi 75773583	Tyr 340	Grigoryan *et al*. (2009c)
Homo sapiens	NSSYFVEWIPNNVK	gi 4507729	Unknown	

In previous studies with purified bovine tubulin, 17 peptides from bovine alpha- and beta-tubulin were found to have been labeled with CPO on tyrosine and lysine. Tyrosine 281 was the most reactive residue in beta-tubulin (Grigoryan *et al*., 2009c). However, no serine was found to be organophosphorylated by CPO in bovine tubulin (Grigoryan *et al*., 2009c). When live mice were treated with chlorpyrifos or CPO, the labeled tubulin residues were tyrosine 281 and serine 338. No other residues were found to be organophosphorylated in mouse tubulin. It is possible that more sensitive methods will detect additional labeled residues in the future.

Table 2 compares the amino acid sequences of bovine and mouse tubulin peptides that include tyrosine 281 and serine 338. The sequence of peptide GSQQY$_{281}$RALTVPELTQQMFDSK is conserved in both species, bovine differing from mouse by virtue of a single conservative change (alanine to serine) at the second position from the C-terminus. Tyrosine 281 is present in both bovine and mouse tubulin. Both bovine beta-tubulin peptide NSSY$_{440}$FVEWIPNNVK and mouse beta-tubulin peptide NS$_{338}$NFVEWIPNNVK have serine at position 338, but only bovine tubulin has tyrosine at position 340. Both peptides are labeled by CPO. The label in bovine tubulin is on tyrosine 440. The difference in target at this locus could reflect the greater nucleophilicity of tyrosine compared to serine.

Seventeen sites on bovine tubulin were labeled with CPO *in vitro*, while only two sites were labeled on mouse tubulin *in vivo*. The larger overall number of labeling sites for bovine tubulin *in vitro* could be partly explained by the fact that the pure bovine tubulin purchased from Cytoskeleton Inc. had been depleted of microtubule-associated proteins before it was treated with CPO. Tyrosine sites available for reaction *in vitro* may be unavailable *in vivo*. The tyrosines might be protected by interaction with other proteins or might already be phosphorylated by kinases (Westermann and Weber, 2003). Prior phosphorylation could mask other potential serine residue targets *in vivo*.

The homologous sequences in human beta-tubulin are nearly identical to those in bovine and mouse beta-tubulin. Sites of labeling on human tubulin are unknown, but they would be expected to be similar to those identified here.

Thin Microtubules and Decreased Proteins on Tubulin Isolated from CPO-treated mice

Thirty-two proteins are listed in Table 1. Eleven of these are forms of tubulin. Two are large proteins (plectin 1 isoform 6 and Titin) with Mowse scores of about 100. These proteins are frequently identified in database searches and may be considered as nonspecific identifications. The remaining 19 proteins appear to copurify with the microtubules. These proteins are recognized as being involved in axonal transport (Maccioni and Cambiazo, 1995; Park *et al*., 2008; Sakamoto *et al*., 2008).

Six proteins in Table 1 were undetectable in microtubules prepared from CPO-treated mice. These were heat-shock protein 84 kDa, alpha-internexin, Myosin Va, dynein cytoplasmic 1 light intermediate chain, cytoskeleton-associated protein 5, and microtubule-associated protein 2 isoform 1. Heat-shock proteins function as molecular chaperones, able to direct folding of cytoskeletal proteins, such as alpha/beta/gamma-tubulin, actin, and centractin (Liang and MacRae, 1997). Internexin is among the five major types of intermediate filament proteins expressed in mature neurons. Alpha-internexin, which is highly expressed during mammalian nervous system development, can coassemble with neurofilament proteins and plays a key role in axonal outgrowth (Lariviere and Julien, 2004). Myosin is involved in fast axonal/dendritic transport and can form a complex with kinesin, a microtubule-based motor. This complex allows long-range movement of vesicles within axons and dendrites on microtubules (Langford, 2002). The formation and maintenance of neuronal synapses are dependent on the active transport of material between the cell body and the axon terminal. Cytoplasmic dynein is one of the motors for microtubule-based axonal transport, and it takes part in regulating the dynamic behavior of microtubules (Hestermann *et al*., 2002; Susalka and Pfister, 2000). Cytoskeleton-associated protein 5 plays a major role in organizing spindle poles. Microtubule-associated protein 2 isoform 1 is a low-molecular weight alternatively spliced variant that is more abundant in embryonic brain than in adult brain (Tucker *et al*., 1988). Thus, the proteins that are missing from microtubules in CPO-treated mouse brain are related to microtubule assembly, structure, stability, and

function. Dissociation of these proteins from the microtubules could account for the abnormally thin microtubules in CPO-treated mice.

Our observation of a decrease in microtubule cosedimenting proteins in response to exposure to CPO is supported by other reports. Prendergast *et al.* (2007) found that CPO treatment of organotypic hippocampal slice cultures from rat brain results in dramatically reduced levels of microtubule-associated protein 2a and 2b. The fluorescence intensity from bound antibody was reduced up to 85% following 3 days of treatment with 1–10μM CPO. However, levels of alpha-tubulin were not altered by CPO exposure, suggesting that the general structure of the microtubules was not destroyed. A proteomic analysis of cultured N2a neuroblastoma cells found that treatment with 10μM diazinon (an OP agent) increased the levels of some proteins, decreased the levels of others, but left tubulin levels unchanged (Harris *et al.*, 2009). It was suggested that diazinon exposure interferes with cytoskeletal networks, disrupting the structure and function of microtubules, microfilaments, and neurofilaments. Reduced levels of the cytoskeletal protein microtubule-associated protein 1B were found in differentiating rat C6 glioma cells following treatment with CPO, thus demonstrating a potent perturbation effect of CPO on the microtubule network (Sachana *et al.*, 2008).

Mechanisms of OP Toxicity Independent of AChE Inhibition

Microtubules are polymers of tubulin dimers that serve in a structural capacity in neurons and as tracks for transporting cell components from the nucleus to the axons and from the axons back to the nucleus. Microtubule-associated proteins bind to tubulin and serve a wide range of functions, including stabilizing, destabilizing, cross-linking, and facilitating interactions between microtubules and other proteins in the cell. Protein binding to microtubules is regulated through phosphorylation. For example, tubulin phosphorylated by calmodulin-dependent protein kinase is not capable of binding to microtubule-associated protein 2 or of polymerizing to microtubules (Wandosell *et al.*, 1986). Detachment of microtubule-associated proteins from the microtubule is regulated by microtubule affinity–regulating kinase. Phosphorylation of the associated proteins and subsequent detachment causes destabilization and destruction of the microtubule. Hyperphosphorylation of the tau protein causes disassembly of microtubules, a phenomenon seen in Alzheimer's disease (Alonso *et al.*, 1994).

Phosphorylation of tubulin and tubulin-associated proteins following challenge with OP agents has been studied *in vitro*, in brain extracts, and *in vivo*, in rats and hens. Choudhary *et al.* (2001) found in rats that dichlorvos induced hyperphosphorylation of tubulin and microtubule-associated protein 2, resulting in destabilization of the microtubule assembly. An increase in phosphorylation of microtubule-associated protein 2 was measured in the brain of hens following a single *in vivo* challenge with diisopropylfluorophosphate (DFP) (Abou-Donia *et al.*, 1993). An increase in the phosphorylation of tubulin, myelin basic protein, and tau was found following *in vitro* DFP treatment of brain extracts (Gupta and Abou-Donia, 1999). The DFP-treated hen had decreased concentrations of tau protein as well as decreased tubulin polymerization (Gupta and Abou-Donia, 1994).

We propose that the reduction in microtubule cosedimenting proteins for microtubules purified from CPO-treated mice resulted from direct organophosphorylation of tubulin by CPO and perhaps from organophosphorylation of the associated proteins as well. It is also possible that enhanced phosphorylation of tubulin and microtubule-associated proteins by kinases such as CaM kinase II was triggered by CPO exposure (Gupta and Abou-Donia, 1999) and that this contributed to the dissociation of some of the microtubule-associated proteins that we observed. We further propose that the dissociation of these vital microtubule-associated proteins resulted in impaired microtubule structure as demonstrated by the significant reduction in their width and height. Such structural alterations imply disruption of microtubule function. These results support a noncholinergic mechanism for OP neurotoxicity in which long-lasting neurotoxicity is due to OP modification of proteins involved in axonal transport.

The question was raised how disruption of axonal transport provides a better explanation of long-lasting neurotoxicity after OP exposure when it is likely that both the persistence of microtubule disruption and of AChE inhibition are short lived? To address this question, we offer the hypothesis developed by Scott Brady and his associates to explain neurodegenerative diseases (Morfini *et al.*, 2009). Their hypothesis is that alterations in phosphorylation-dependent intracellular signaling mechanisms result in alterations of axonal transport. Dysregulation of axonal transport causes axons to lose connectivity to synapses and to slowly die back. The consequence is a slow neurodegeneration. The abnormality that initiates these events in diseases such as Alzheimer's and Huntington's is a mutation. We propose that phosphorylation abnormalities can also be initiated by covalent binding of OP. The present work demonstrates covalent binding by OP. Other workers have shown that treatment with OP leads to hyperphosphorylation of neurofilaments, tau, calcium/cyclic AMP response element binding protein, tubulin, and microtubule-associated protein 2 (Choudhary *et al.*, 2001; Gupta and Abou-Donia, 1999; Gupta *et al.*, 1997; Schuh *et al.*, 2002) and to disruption of adenylyl cyclase signaling and serotonin-mediated signal transduction (Aldridge *et al.*, 2003; Song *et al.*, 1997). Thus, we propose a mechanism in which low-dose exposure to OP disrupts axonal transport for a sufficient length of time to initiate an irreversible degradation of the neuron, which in turn leads to permanent loss of neuronal function.

FUNDING

U.S. Army Medical Research and Materiel Command (W81XWH-07-2-0034); the National Institutes of Health

(NIH) (U01 NS058056 and P30CA36727); NIH (SIG program), the UNMC Program of Excellence, the Nebraska Research Initiative; Mass spectra were obtained with the support of the Mass Spectrometry; Proteomics Core Facility at the University of Nebraska Medical Center.

ACKNOWLEDGMENTS

Nanoimages were obtained with the support of L.S., codirector, and Dr Yuri L. Lyubchenko, director of the Nanoimaging Core Facility at the University of Nebraska Medical Centerin the Department of Pharmaceutical Sciences. The Nanoimaging Core.

REFERENCES

Abou-Donia, M. B., Viana, M. E., Gupta, R. P., and Anderson, J. K. (1993). Enhanced calmodulin binding concurrent with increased kinase-dependent phosphorylation of cytoskeletal proteins following a single subcutaneous injection of diisopropyl phosphorofluoridate in hens. *Neurochem. Int.* **22,** 165–173.

Aldridge, J. E., Seidler, F. J., Meyer, A., Thillai, I., and Slotkin, T. A. (2003). Serotonergic systems targeted by developmental exposure to chlorpyrifos: effects during different critical periods. *Environ. Health Perspect.* **111,** 1736–1743.

Alonso, A. C., Zaidi, T., Grundke-Iqbal, I., and Iqbal, K. (1994). Role of abnormally phosphorylated tau in the breakdown of microtubules in Alzheimer disease. *Proc. Natl. Acad. Sci. U.S.A.* **91,** 5562–5566.

Amitai, G., Moorad, D., Adani, R., and Doctor, B. P. (1998). Inhibition of acetylcholinesterase and butyrylcholinesterase by chlorpyrifos-oxon. *Biochem. Pharmacol.* **56,** 293–299.

Choudhary, S., Joshi, K., and Gill, K. D. (2001). Possible role of enhanced microtubule phosphorylation in dichlorvos induced delayed neurotoxicity in rat. *Brain Res.* **897,** 60–70.

Conde, C., and Caceres, A. (2009). Microtubule assembly, organization and dynamics in axons and dendrites. *Nat. Rev. Neurosci.* **10,** 319–332.

Friden, B., and Wallin, M. (1991). Dependency of microtubule-associated proteins (MAPs) for tubulin stability and assembly; use of estramustine phosphate in the study of microtubules. *Mol. Cell. Biochem.* **105,** 149–158.

Gearhart, D. A., Sickles, D. W., Buccafusco, J. J., Prendergast, M. A., and Terry, A. V., Jr. (2007). Chlorpyrifos, chlorpyrifos-oxon, and diisopropylfluorophosphate inhibit kinesin-dependent microtubule motility. *Toxicol. Appl. Pharmacol.* **218,** 20–29.

Grigoryan, H., Li, B., Anderson, E. K., Xue, W., Nachon, F., Lockridge, O., and Schopfer, L. M. (2009a). Covalent binding of the organophosphorus agent FP-biotin to tyrosine in eight proteins that have no active site serine. *Chem. Biol. Interact.* **180,** 492–498. PMCID:2700782.

Grigoryan, H., Li, B., Xue, W., Grigoryan, M., Schopfer, L. M., and Lockridge, O. (2009b). Mass spectral characterization of organophosphate-labeled lysine in peptides. *Anal. Biochem.* **394,** 92–100.

Grigoryan, H., and Lockridge, O. (2009). Nanoimages show disruption of tubulin polymerization by chlorpyrifos oxon: implications for neurotoxicity. *Toxicol. Appl. Pharmacol.* **240,** 143–148. NIHMS:134468.

Grigoryan, H., Schopfer, L. M., Peeples, E. S., Duysen, E. G., Grigoryan, M., Thompson, C. M., and Lockridge, O. (2009c). Mass spectrometry identifies multiple organophosphorylated sites on tubulin. *Toxicol. Appl. Pharmacol.* **240,** 149–158.

Grigoryan, H., Schopfer, L. M., Thompson, C. M., Terry, A. V., Masson, P., and Lockridge, O. (2008). Mass spectrometry identifies covalent binding of soman, sarin, chlorpyrifos oxon, diisopropyl fluorophosphate, and FP-biotin to tyrosines on tubulin: a potential mechanism of long term toxicity by organophosphorus agents. *Chem. Biol. Interact.* **175,** 180–186.

Gupta, R. P., Abdel-Rahman, A., Wilmarth, K. W., and Abou-Donia, M. B. (1997). Alteration in neurofilament axonal transport in the sciatic nerve of the diisopropyl phosphorofluoridate (DFP)-treated hen. *Biochem. Pharmacol.* **53,** 1799–1806.

Gupta, R. P., and Abou-Donia, M. B. (1994). In vivo and in vitro effects of diisopropyl phosphorofluoridate (DFP) on the rate of hen brain tubulin polymerization. *Neurochem. Res.* **19,** 435–444.

Gupta, R. P., and Abou-Donia, M. B. (1999). Tau phosphorylation by diisopropyl phosphorofluoridate (DFP)-treated hen brain supernatant inhibits its binding with microtubules: role of Ca2+/Calmodulin-dependent protein kinase II in tau phosphorylation. *Arch. Biochem. Biophys.* **365,** 268–278.

Harris, W., Sachana, M., Flaskos, J., and Hargreaves, A. J. (2009). Proteomic analysis of differentiating neuroblastoma cells treated with sub-lethal neurite inhibitory concentrations of diazinon: identification of novel biomarkers of effect. *Toxicol. Appl. Pharmacol.* **240,** 159–165.

Hestermann, A., Rehberg, M., and Graf, R. (2002). Centrosomal microtubule plus end tracking proteins and their role in Dictyostelium cell dynamics. *J. Muscle Res. Cell. Motil.* **23,** 621–630.

Kawada, T., Katsumata, M., Suzuki, H., Li, Q., Inagaki, H., Nakadai, A., Shimizu, T., Hirata, K., and Hirata, Y. (2005). Insomnia as a sequela of sarin toxicity several years after exposure in Tokyo subway trains. *Percept. Mot. Skills.* **100,** 1121–1126.

Langford, G. M. (2002). Myosin-V, a versatile motor for short-range vesicle transport. *Traffic* **3,** 859–865.

Lariviere, R. C., and Julien, J. P. (2004). Functions of intermediate filaments in neuronal development and disease. *J. Neurobiol.* **58,** 131–148.

Li, B., Schopfer, L. M., Grigoryan, H., Thompson, C. M., Hinrichs, S. H., Masson, P., and Lockridge, O. (2009). Tyrosines of human and mouse transferrin covalently labeled by organophosphorus agents: a new motif for binding to proteins that have no active site serine. *Toxicol. Sci.* **107,** 144–155. PMCID:2638647.

Liang, P., and MacRae, T. H. (1997). Molecular chaperones and the cytoskeleton. *J. Cell. Sci.* **110**(Pt 13), 1431–1440.

Lyubchenko, Y. L., and Shlyakhtenko, L. S. (2009). AFM for analysis of structure and dynamics of DNA and protein-DNA complexes. *Methods* **47,** 206–213.

Maccioni, R. B., and Cambiazo, V. (1995). Role of microtubule-associated proteins in the control of microtubule assembly. *Physiol. Rev.* **75,** 835–864.

McDonough, J. H., Jr, and Shih, T. M. (1997). Neuropharmacological mechanisms of nerve agent-induced seizure and neuropathology. *Neurosci. Biobehav. Rev.* **21,** 559–579.

Morfini, G. A., Burns, M., Binder, L. I., Kanaan, N. M., LaPointe, N., Bosco, D. A., Brown, R. H., Jr, Brown, H., Tiwari, A., Hayward, L., *et al.* (2009). Axonal transport defects in neurodegenerative diseases. *J. Neurosci.* **29,** 12776–12786.

Park, H., Kim, M., and Fygenson, D. K. (2008). Tau-isoform dependent enhancement of taxol mobility through microtubules. *Arch. Biochem. Biophys.* **478,** 119–126.

Peeples, E. S., Schopfer, L. M., Duysen, E. G., Spaulding, R., Voelker, T., Thompson, C. M., and Lockridge, O. (2005). Albumin, a new biomarker of organophosphorus toxicant exposure, identified by mass spectrometry. *Toxicol. Sci.* **83,** 303–312.

Perkins, D. N., Pappin, D. J., Creasy, D. M., and Cottrell, J. S. (1999). Probability-based protein identification by searching sequence databases using mass spectrometry data. *Electrophoresis* **20,** 3551–3567.

Prendergast, M. A., Self, R. L., Smith, K. J., Ghayoumi, L., Mullins, M. M., Butler, T. R., Buccafusco, J. J., Gearhart, D. A., and Terry, A. V., Jr. (2007). Microtubule-associated targets in chlorpyrifos oxon hippocampal neurotoxicity. *Neuroscience* **146,** 330–339.

Read, R. W., Riches, J. R., Stevens, J. A., Stubbs, S. J., and Black, R. M. (2010). Biomarkers of organophosphorus nerve agent exposure: comparison of phosphylated butyrylcholinesterase and phosphylated albumin after oxime therapy. *Arch. Toxicol.* **84,** 25–36.

Rishal, I., Michaelevski, I., Rozenbaum, M., Shinder, V., Medzihradszky, K. F., Burlingame, A. L., and Fainzilber, M. (2010). Axoplasm isolation from peripheral nerve. *Dev. Neurobiol.* **70,** 126–133.

Sachana, M., Flaskos, J., Sidiropoulou, E., Yavari, C. A., and Hargreaves, A. J. (2008). Inhibition of extension outgrowth in differentiating rat C6 glioma cells by chlorpyrifos and chlorpyrifos oxon: effects on microtubule proteins. *Toxicol. In Vitro* **22,** 1387–1391.

Sakamoto, T., Uezu, A., Kawauchi, S., Kuramoto, T., Makino, K., Umeda, K., Araki, N., Baba, H., and Nakanishi, H. (2008). Mass spectrometric analysis of microtubule co-sedimented proteins from rat brain. *Genes Cells* **13,** 295–312.

Salvi, R. M., Lara, D. R., Ghisolfi, E. S., Portela, L. V., Dias, R. D., and Souza, D. O. (2003). Neuropsychiatric evaluation in subjects chronically exposed to organophosphate pesticides. *Toxicol. Sci.* **72,** 267–271.

Sams, C., Cocker, J., and Lennard, M. S. (2004). Biotransformation of chlorpyrifos and diazinon by human liver microsomes and recombinant human cytochrome P450s (CYP). *Xenobiotica* **34,** 861–873.

Schuh, R. A., Lein, P. J., Beckles, R. A., and Jett, D. A. (2002). Noncholinesterase mechanisms of chlorpyrifos neurotoxicity: altered phosphorylation of Ca2+/cAMP response element binding protein in cultured neurons. *Toxicol. Appl. Pharmacol.* **182,** 176–185.

Shelanski, M. L., Gaskin, F., and Cantor, C. R. (1973). Microtubule assembly in the absence of added nucleotides. *Proc. Natl. Acad. Sci. U.S.A.* **70,** 765–768.

Shlyakhtenko, L. S., Gall, A. A., Filonov, A., Cerovac, Z., Lushnikov, A., and Lyubchenko, Y. L. (2003). Silatrane-based surface chemistry for immobilization of DNA, protein-DNA complexes and other biological materials. *Ultramicroscopy* **97,** 279–287.

Song, X., Seidler, F. J., Saleh, J. L., Zhang, J., Padilla, S., and Slotkin, T. A. (1997). Cellular mechanisms for developmental toxicity of chlorpyrifos: targeting the adenylyl cyclase signaling cascade. *Toxicol. Appl. Pharmacol.* **145,** 158–174.

Srivastava, A. K., Gupta, B. N., Bihari, V., Mathur, N., Srivastava, L. P., Pangtey, B. S., Bharti, R. S., and Kumar, P. (2000). Clinical, biochemical and neurobehavioural studies of workers engaged in the manufacture of quinalphos. *Food Chem. Toxicol.* **38,** 65–69.

Susalka, S. J., and Pfister, K. K. (2000). Cytoplasmic dynein subunit heterogeneity: implications for axonal transport. *J. Neurocytol.* **29,** 819–829.

Tang, J., Cao, Y., Rose, R. L., Brimfield, A. A., Dai, D., Goldstein, J. A., and Hodgson, E. (2001). Metabolism of chlorpyrifos by human cytochrome P450 isoforms and human, mouse, and rat liver microsomes. *Drug Metab. Dispos.* **29,** 1201–1204.

Terry, A. V., Jr, Gearhart, D. A., Beck, W. D., Jr, Truan, J. N., Middlemore, M. L., Williamson, L. N., Bartlett, M. G., Prendergast, M. A., Sickles, D. W., and Buccafusco, J. J. (2007). Chronic, intermittent exposure to chlorpyrifos in rats: protracted effects on axonal transport, neurotrophin receptors, cholinergic markers, and information processing. *J. Pharmacol. Exp. Ther.* **322,** 1117–1128.

Tierno, M. B., Kitchens, C. A., Petrik, B., Graham, T. H., Wipf, P., Xu, F. L., Saunders, W. S., Raccor, B. S., Balachandran, R., Day, B. W., *et al.* (2009). Microtubule binding and disruption and induction of premature senescence by disorazole C(1). *J. Pharmacol. Exp. Ther.* **328,** 715–722.

Tucker, R. P., Binder, L. I., Viereck, C., Hemmings, B. A., and Matus, A. I. (1988). The sequential appearance of low- and high-molecular-weight forms of MAP2 in the developing cerebellum. *J. Neurosci.* **8,** 4503–4512.

Wandosell, F., Serrano, L., Hernandez, M. A., and Avila, J. (1986). Phosphorylation of tubulin by a calmodulin-dependent protein kinase. *J. Biol. Chem.* **261,** 10332–10339.

Westermann, S., and Weber, K. (2003). Post-translational modifications regulate microtubule function. *Nat. Rev. Mol. Cell Biol.* **4,** 938–947.

Wiederin, J., Rozek, W., Duan, F., and Ciborowski, P. (2009). Biomarkers of HIV-1 associated dementia: proteomic investigation of sera. *Proteome Sci.* **7,** 8.

Yamasue, H., Abe, O., Kasai, K., Suga, M., Iwanami, A., Yamada, H., Tochigi, M., Ohtani, T., Rogers, M. A., Sasaki, T., *et al.* (2007). Human brain structural change related to acute single exposure to sarin. *Ann. Neurol.* **61,** 37–46.

Yanagisawa, N., Morita, H., and Nakajima, T. (2006). Sarin experiences in Japan: acute toxicity and long-term effects. *J. Neurol. Sci.* **249,** 76–85.